METHODOLOGY

Stochastic variational variable selection for high-dimensional microbiome data

Tung Dang[1], Kie Kumaishi[2], Erika Usui[2], Shungo Kobori[2], Takumi Sato[2], Yusuke Toda[1], Yuji Yamasaki[3], Hisashi Tsujimoto[3], Yasunori Ichihashi[2] and Hiroyoshi Iwata[1*]

*Correspondence: hiroiwata@g.ecc.u-tokyo.ac.jp
[1]Graduate School of Agricultural and Life Sciences, The University of Tokyo, Tokyo, Japan
Full list of author information is available at the end of the article

Abstract

Background: The rapid and accurate identification of a minimal-size core set of representative microbial species plays an important role in the clustering of microbial community data and interpretation of the clustering results. However, the huge dimensionality of microbial metagenomics data sets is a major challenge for the existing methods such as Dirichlet multinomial mixture (DMM) models. In the framework of the existing methods, computational burdens for identifying a small number of representative species from a huge number of observed species remain a challenge.

Results: We proposed a novel framework to improve the performance of the widely used DMM approach by combining three ideas: (i) We extended the finite DMM model to the infinite case, via the consideration of Dirichlet process mixtures and estimate the number of clusters as a random variables. (ii) We proposed an indicator variable to identify representative operational taxonomic units that substantially contribute to the differentiation among clusters. (iii) To address the computational burdens of the high-dimensional microbiome data, we proposed are a stochastic variational inference, which approximates the posterior distribution using a controllable distribution called variational distribution, and stochastic optimization algorithms for fast computation. With the proposed method named stochastic variational variable selection (SVVS), we analyzed the root microbiome data collected in our soybean field experiment and the human gut microbiome data from three published data sets of large-scale case-control studies.

Conclusions: SVVS demonstrated a better performance and significantly faster computation than existing methods in all cases of testing data sets. In particular, SVVS is the only method that can analyze the massive high-dimensional microbial data with above 50,000 microbial species and 1,000 samples. Furthermore, it was suggested that microbial species selected as a core set played important roles in the recent microbiome studies.

Keywords: variational inference; stochastic optimization; Bayesian infinite mixture model; variable selection; drought irrigation; environmental and human microbiome

Background

The development of metagenomic high-throughput sequencing technologies has provided a rapid and sensitive method for the discovery of the human microbiome and soil microbial communities. Accordingly, our understanding of the impact of the gut microbiota on the human body [1, 2] and the significance of bacterial ecology in

the global biogeochemical nutrient cycle [3] is meaningfully expanding. There are two major types of microbial metagenomics data that include the 16S ribosomal RNA gene and shotgun metagenomics. In this study, we focused on the analysis of the 16S ribosomal RNA gene as an example, although shotgun metagenomics data can be analyzed in a relatively similar manner. One of the standard approaches is that the 16S rRNA gene of the bacteria in the samples is transformed into operational taxonomic units (OTUs) by using a preprocessing method, such as QIIME [4]. Next, using the transformed data sets, we are aiming to identify the microbial composition that differs among multiple groups of communities and to elucidate the relationship between these groups on one hand and terrestrial ecosystems, human health, etc. on the other.

Considering the heterogeneous pattern of sample-to-sample variability in the microbiome data, various model-based approaches have been proposed for clustering microbiome samples. The finite Dirichlet multinomial mixture (DMM) model is one of the most widely used methods [5]. The main ideas behind the DMM model are as follows: first, a multinomial sampling scheme is adopted to OTU count data, and then a mixture of Dirichlet components is considered as the natural prior for the parameters of the multinomial distribution. This approach helps avoid the disadvantages of previous methods assuming that all samples in a cohort are generated from a single community profile and allows each community to be assumed to be a mixture of multiple communities, which can be described by a vector generated by one of the finite Dirichlet mixture components with different hyperparameters. Therefore, the flexibility of the DMM model with respect to model dimensionality makes it better for capturing many different subcommunity structures. Such methods are of great practical importance and have been used to assess the potential associations of the microbiome community in human health and disease studies [6, 7], microbiome genome-wide association studies [8], and animal microbiomes studies [9].

The first step in analysis with a conventional DMM model is to decide the numbers of microbiome clusters, i.e., metacommunities biologically required for explaining the observations. A fully Bayesian model selection through Laplace approximation [5] is proposed to consider all possible values of the numbers of metacommunities up to a certain maximum value. The optimization of the number via this approach is, however, computationally prohibitive and may cause poor performance when the dimensionality of the microbiome data sets is high. Moreover, it is worth mentioning that all OTUs in the DMM model are assumed to be equally significant for the clustering analysis. However, it is not realistic in practical analysis since, of the thousands or tens of thousands of OTUs, a large number might be irrelevant and might not significantly contribute to the identification (or characterization) of the microbiome clusters.

Recently, various potential approaches have been proposed to estimate the parameters of a nonparametric Bayesian unsupervised variable selection in the field of computer science, such as a hybrid framework based on a combination of Gibbs sampling and Metropolis-Hastings algorithms that appropriately accounts for the conditional independence relationships between latent variables and model parameters [10, 11]. One of the important advantages of the MCMC solutions is the yielding

of a robust and stable estimation by including the observed data into the computational processes. However, the computational burden of the MCMC solutions is prohibitive for inference given the large dimensionality of microbial metagenomics data sets, and it can be very difficult to diagnose their convergence.

In this study, we proposed a novel approach that overcomes the challenges described above and achieves the feasible computational ability for a personal computer. The main contributions of this study are three-fold. First, we extended the finite DMM model by proposing a Bayesian nonparametric approach, which was based on a countable infinite mixture model coupled with variable selection. In our approach, the number of clusters (metacommunities) was not fixed a priori and was itself a free parameter of the inference under the truncated stick-breaking representation of the Dirichlet process prior on the space of mixture metacommunities [12, 13, 14]. This solution could overcome the difficulty of choosing the appropriate number of clusters based on the data. Moreover, our method enabled the estimation of the significant contributions of OTUs in order to detect a minimal-size core set of OTUs that characterize clusters and could maximize the identification ability of the clusters. Secondly, to overcome the currently computational difficulties related to deterministic learning and MCMC approaches, we proposed a stochastic variational inference (SVI) method [15, 16, 17] , which was originally used in statistical physics to approximate intractable integrals and has been successfully used in a wide variety of applications for analyzing the large data sets related to population genetics [18, 19] and phylogenetics [20, 21, 22]. It is noteworthy that the analytically tractable solution for calculating the posterior distributions is provided in order to avoid the expensive computations of the numerical approximations in the MCMC approaches [23, 24]. Finally, we applied the proposed approaches to analyze a 16S rRNA gene amplicon sequencing environmental microbiome data of soybean genetic resources collected in our field experiment. The data set included 196 and 197 rhizosphere samples, which contained 888 OTUs, from a drought irrigation and control conditions, respectively. Moreover, our proposed approach was applied to three published case-control 16S rRNA gene amplicon sequencing human gut microbiome data sets [25, 26, 27]. Specifically, the first database included 3,347 OTUs for *Clostridium difficile* infection (CDI) from 338 individuals including 89 individuals with CDI (cases), 89 with diarrhea who tested negative for CDI (diarrhea controls), and 155 non-diarrhea controls [25]. Moreover, inflammatory bowel disease (IBD) data and obesity (OB) data provided a large number of OTUs (approximately 10,000 and 50,000, respectively) that challenge the computational capability of stochastic variational variable selection (SVVS) [26, 27].

Methods and materials

The finite Dirichlet multinomial mixture model

First, the finite DMM model that described the heterogeneity of the cross-sample variability among the microbiome species was briefly reviewed [5]. This model allowed the data set that is generated by a mixture of K metacommunities instead of a single metacommunity. The key ideas behind the DMM model are explained below.

Given a microbiome dataset consisting of N community samples and S OTUs (or species), the observed count of the ith community for j^{th} OTU was denoted as X_{ij} ($i = 1, \ldots, N$; $j = 1, \ldots, S$). The total number of counts (i.e., sequence reads) from the ith community sample is $J_i = \sum_{j=1}^{S} X_{ij}$. The DMM model [5] considered a vector $\overrightarrow{X_i} = (X_{i1}, \ldots, X_{iS})$, drawn from a multinomial distribution with community vector $\overrightarrow{p_i} = (p_{i1}, \ldots, p_{iS})$ as follows:

$$
\begin{aligned}
&p\left(\overrightarrow{X_i}|J_i, \overrightarrow{p_i}\right) = Multi\left(J_i, \overrightarrow{p_i}\right) \\
&p\left(\overrightarrow{p_i}|\boldsymbol{\pi}, \boldsymbol{\alpha}\right) = \sum_{k=1}^{K} \pi_k Dir(\overrightarrow{p_i}|\overrightarrow{\alpha_k})
\end{aligned} \tag{1}
$$

where p_{ij} is the probability that a single read in the ith community belongs to the jth OTU, $\overrightarrow{\alpha_k} = (\alpha_{k1}, \ldots, \alpha_{kS})$ are the parameters of the Dirichlet distribution representing k^{th} metacommunity (or cluster), and $\boldsymbol{\pi} = (\pi_1, \ldots, \pi_K)$ represents the mixing coefficients with $\sum_{k=1}^{K} \pi_k = 1$, $\pi_k \geq 0$ for $k \in (1, \ldots, K)$. It is noteworthy that the finite DMM model examined the case where the number of metacommunities, K, was considered to be fixed. Each sample was assumed to be a draw from each unique community vector $\overrightarrow{p_i}$ that was derived from one of the K metacommunities. Therefore, the equation (1) can be rewritten by marginalizing the multinomial parameters as follow [5]:

$$
p\left(\boldsymbol{X}|\boldsymbol{\pi}, \boldsymbol{\alpha}\right) = \sum_{k=1}^{K} \pi_k \left[\prod_{i=1}^{N} \left(\frac{B\left(\overrightarrow{\alpha_k} + \overrightarrow{X_i}\right)}{B\left(\overrightarrow{\alpha_k}\right)} J_i! \prod_{j=1}^{S} \frac{1}{X_{ij}!}\right)\right] \tag{2}
$$

where the function B is the multinomial Beta function $B\left(\overrightarrow{\alpha_k}\right) = \frac{\prod_{j=1}^{S} \Gamma(\alpha_{kj})}{\Gamma\left(\sum_{j=1}^{S} \alpha_{kj}\right)}$ and $B\left(\overrightarrow{\alpha_k} + \overrightarrow{X_i}\right) = \frac{\prod_{j=1}^{S} \Gamma(\alpha_{kj} + X_{ij})}{\Gamma\left(\sum_{j=1}^{S} (\alpha_{kj} + X_{ij})\right)}$

The infinite Dirichlet multinomial mixture model with variable selection

The goal was to consider the number of metacommunities (K) to be a random variable. To do this, it was assumed that the prior distribution of the mixing coefficients $\boldsymbol{\pi}$ followed a Dirichlet process prior [12]. The stick-breaking representation [13] [14], which is a straightforward constructive definition of the Dirichlet process, was adopted to construct the infinite DMM model proposed in this study. It was defined as follows:

$$
\begin{aligned}
&p\left(\gamma_k\right) = Beta\left(1, \nu\right) \\
&\pi_k = \gamma_k \prod_{k'=1}^{k-1} \left(1 - \gamma_{k'}\right)
\end{aligned}
$$

where π_k is the mixing proportions of an infinite number of successively broken sticks; the unit length of sticks that correspond to the kth metacommunity (or cluster), γ_k with ($k \in [1, \ldots, K]$), and ν represents the total mass parameter of the Dirichlet process. It was assumed that each community sample $\overrightarrow{X_i}$ was generated

from the DMM model with a countably infinite of number of clusters (or metacommunities). Therefore, the equation (2) was rewritten as

$$p\left(\overrightarrow{X_i}|\boldsymbol{\pi},\boldsymbol{\alpha}\right)=\sum_{k=1}^{\infty}\pi_k\left(\frac{B\left(\overrightarrow{\alpha_k}+\overrightarrow{X_i}\right)}{B\left(\overrightarrow{\alpha_k}\right)}J_i!\prod_{j=1}^{S}\frac{1}{X_{ij}!}\right) \tag{3}$$

Next, we introduced the allocation variable $\overrightarrow{Z_i}=(Z_{i1},Z_{i2},\ldots)$, such $Z_{ik}\in[0,1]$ and $Z_{ik}=1$ if $\overrightarrow{X_i}$ belongs to the metacommunity k (i.e., the cluster k) and 0, otherwise. Moreover, all OTUs in the DMM model were assumed to be equally important for the clustering of microbial community data. However, this is not realistic in microbiome studies since a large number of microbiome species (which can be reflected on OTUs) and functions might be irrelevant and significantly influence the performance of clustering algorithms [28]. In order to overcome this problem, it is proposed that the count of a given OTU, X_{ij}, is generated from a mixture of two Dirichlet-multinomial distributions: the first one is assumed to generate a core set of the most significant microbial OTUs and is different for each single metacommunity; the second one is assumed to generate the unimportant OTUs and is common to all multiple metacommunities. Thus, we can write the likelihood of the observed microbiome data set $\boldsymbol{X}$ following the infinite DMM model with microbiome OTUs selection as:

$$p\left(\boldsymbol{X}|\boldsymbol{Z},\boldsymbol{\phi},\boldsymbol{\alpha},\boldsymbol{\beta}\right)=\prod_{i=1}^{N}\prod_{k=1}^{\infty}\left[\begin{array}{c}\left(\frac{B\left(\overrightarrow{\alpha_k}+\overrightarrow{X_i}\right)}{B\left(\overrightarrow{\alpha_k}\right)}J_i!\prod_{j=1}^{S}\frac{1}{X_{ij}!}\right)^{\phi_{ij}}\\ \left(\frac{B\left(\boldsymbol{\beta}+\overrightarrow{X_i}\right)}{B\left(\boldsymbol{\beta}\right)}J_i!\prod_{j=1}^{S}\frac{1}{X_{ij}!}\right)^{1-\phi_{ij}}\end{array}\right]^{Z_{ik}} \tag{4}$$

where ϕ_{ij} is a indicator variable, such that $\phi_{ij}=1$ indicates that the jth OTU of ith community is important in the kth cluster and follows a Dirichlet-multinomial distribution with $\boldsymbol{\alpha}$ parameter and $\phi_{ij}=0$ denotes that the jth OTU of ith community is unimportant in the kth cluster and follows a Dirichlet-multinomial distribution with $\boldsymbol{\beta}$ parameter. $B\left(\overrightarrow{\alpha_k}\right)$ and $B\left(\overrightarrow{\alpha_k}+\overrightarrow{X_i}\right)$ are the multinomial Beta functions for a core set of the OTUs significantly representing the cluster. In the case of unimportant species, multinomial Beta functions are $B\left(\boldsymbol{\beta}\right)=\frac{\prod_{j=1}^{S}\Gamma(\beta_j)}{\Gamma\left(\sum_{j=1}^{S}\beta_j\right)}$ and $B\left(\boldsymbol{\beta}+\overrightarrow{X_i}\right)=\frac{\prod_{j=1}^{S}\Gamma(\beta_j+X_{ij})}{\Gamma\left(\sum_{j=1}^{S}(\beta_j+X_{ij})\right)}$. The prior distribution for the indicator variable of microbiome selection $\boldsymbol{\phi}$ is defined as follows:

$$p\left(\boldsymbol{\phi}|\boldsymbol{\epsilon}\right)=\prod_{i=1}^{N}\prod_{j=1}^{S}\epsilon_{j_1}^{\phi_{ij}}\epsilon_{j_2}^{1-\phi_{ij}}$$

where each ϕ_{ij} follows a Bernoulli distribution such that $p\left(\phi_{ij}=1\right)=\epsilon_{j_1}$ and $p\left(\phi_{ij}=0\right)=\epsilon_{j_2}$ with $\epsilon_{j_1}+\epsilon_{j_2}=1$ [11]. Furthermore, the Dirichlet distributions are considered for $(\epsilon_{j_1},\epsilon_{j_2})$ with the hyperparameters (ξ_1,ξ_2) [29]. The prior distributions of $\boldsymbol{\alpha}$ and $\boldsymbol{\beta}$ follow the Dirichlet distributions with hyperparameters $\boldsymbol{\zeta}$ and $\boldsymbol{\eta}$.

The stochastic variational variable selection approach

Here, we proposed a SVI method [15] [16] [17] in order to learn the infinite DMM model with the selection of variables (i.e., the counts of OTUs). The basic idea of variational learning in the Bayesian framework is to approximate the posterior distribution by a computationally tractable function called the variational distribution. The variational parameter, which specifies the variational distribution, is estimated by minimizing the Kullback-Leibler (KL) divergence of the posterior distribution to the variational distribution. As a result, the posterior distribution is estimated by numerical optimization with the triggering of the simulation approaches, such as MCMC algorithms.

Given the observed count data set $\boldsymbol{X}$, the infinite DMM model has a set of parameters (Ξ), which consists of the unit length of the stick ($\boldsymbol{\gamma}$), the allocation variable ($\boldsymbol{Z}$) of the Dirichlet prior, the indicator variable of OTUs selection ($\boldsymbol{\phi}$), and the Dirichlet parameters ($\boldsymbol{\alpha}, \boldsymbol{\beta}$). Variational inference approximates the true intractable posterior distribution $p(\Xi|\boldsymbol{X})$ by an element of a tractable family of probability distributions $q(\Xi|\Theta)$ called the variational distribution. This distribution is parameterized by the free parameters, called variational parameters Θ. The variational inference estimates these parameters to find a distribution close to the true intractable posterior distribution of interest. The distance between the distributions $p(\Xi|\boldsymbol{X})$ and $q(\Xi|\Theta)$ is evaluated with the KL divergence represented as follows:

$$\begin{aligned}
&\mathrm{KL}\left[q\left(\Xi|\Theta\right)|p\left(\Xi|\boldsymbol{X}\right)\right] \\
&= \mathrm{E_q}\left[\log\left(q\left(\Xi|\Theta\right)\right)\right] - \mathrm{E_q}\left[\log\left(p\left(\Xi|\boldsymbol{X}\right)\right)\right] \\
&= \mathrm{E_q}\left[\log\left(q\left(\Xi|\Theta\right)\right)\right] - \mathrm{E_q}\left[\log\left(p\left(\Xi,\boldsymbol{X}\right)\right)\right] + \log\left(p\left(\boldsymbol{X}\right)\right)
\end{aligned} \tag{5}$$

The log marginal probability $\log(p(\boldsymbol{X}))$ in equation (5), which is the cause of computational difficulty in the Bayesian framework, can be treated as a constant term in the numerical optimization for estimating the variational parameters as follows:

$$\Theta^* = \mathrm{argmin}\mathrm{KL}\left[q\left(\Xi|\Theta\right)|p\left(\Xi|\boldsymbol{X}\right)\right]$$

Besides, the term $\log(p(\boldsymbol{X}))$ can be decomposed as $\log(p(\boldsymbol{X})) = \mathcal{L}[q(\Xi|\Theta)] + \mathrm{KL}[q(\Xi|\Theta)|p(\Xi|\boldsymbol{X})]$. The variational inference maximizes the computational feasible target function as follows:

$$\mathcal{L}\left[q\left(\Xi|\Theta\right)\right] = \mathrm{E_q}\left[\log\left(p\left(\Xi,\boldsymbol{X}\right)\right)\right] - \mathrm{E_q}\left[\log\left(q\left(\Xi|\Theta\right)\right)\right] \tag{6}$$

where equation (6) is called Evidence Lower Bound (ELBO) [15]. $\mathcal{L}[q(\Xi|\Theta)]$ can be considered as a lower bound for $\log(p(\boldsymbol{X}))$. Perceptibly, the maximization of ELBO equals the minimization of KL divergence, that is, when the variational distribution $q(\Xi|\Theta)$ approximates the true posterior distribution $p(\Xi|\boldsymbol{X})$. However, the fact indices of the computation of the true posterior distribution are intractable and the direct application of the variational framework is infeasible. Therefore,

the mean-field framework was adopted in order to factorize the posterior distribution into disjoint tractable distributions. According to a factorization assumption of mean-field variational approximations [16] [17], each variable of the variational distribution $q(\Xi|\Theta)$ is independent. Furthermore, we considered the truncated stick-breaking representations for the DMM model at the largest possible of a number of metacommunities (or clusters) $\mathrm{K}_{\max}$. It is worth mentioning that the variational framework can optimize the value of truncation $\mathrm{K}_{\max}$ because it becomes a variational parameter. The family of variational distribution in the infinite DMM model with the selection of representative OTUs can be written as follows:

$$\begin{aligned}
&q(\boldsymbol{Z}, \boldsymbol{\phi}, \boldsymbol{\gamma}, \boldsymbol{\epsilon}, \boldsymbol{\alpha}, \boldsymbol{\beta}|\Theta) \\
&= \prod_{i=1}^{N} \prod_{k=1}^{K_{max}} q(Z_{ik}|r_{ik}) \times \prod_{k=1}^{K_{max}} q\left(\gamma_k|\vartheta_k, \vartheta_k^{'}\right) \times \prod_{i=1}^{N} \prod_{j=1}^{S} q(\phi_{ij}|f_{ij}) \\
&\times \prod_{j=1}^{S} q(\epsilon_j|\xi^*) \times \prod_{k=1}^{K_{max}} \prod_{j=1}^{S} q\left(\alpha_{kj}|\lambda_{kj}^*\right) \times \prod_{j=1}^{S} q\left(\beta_j|\iota_j^*\right)
\end{aligned} \tag{7}$$

where:

$$\begin{aligned}
&q(Z_{ik}|r_{ik}) = \text{Multinomial}(Z_{ik}|r_{ik}) \\
&q\left(\gamma_k|\vartheta_k, \vartheta_k^{'}\right) = \text{Beta}\left(\gamma_k|\vartheta_k, \vartheta_k^{'}\right) \\
&q(\phi_{ij}|f_{ij}) = f_{ij}^{\phi_{ij}}(1-f_{ij})^{1-\phi_{ij}} \\
&q(\epsilon_j|\xi^*) = \text{Dirichlet}(\epsilon_j|\xi^*) \\
&q\left(\alpha_{kj}|\lambda_{kj}^*\right) = \text{Dirichlet}\left(\alpha_{kj}|\lambda_{kj}^*\right) \\
&q\left(\beta_j|\iota_j^*\right) = \text{Dirichlet}\left(\beta_j|\iota_j^*\right)
\end{aligned} \tag{8}$$

The set of free variational parameters Θ includes $r_{ik}, \vartheta_k, \vartheta_k^{'}, f_{ij}, \xi^*, \lambda_{kj}^*, \iota_j^*$. We considered the variational distributions from exponential families in order to guarantee the tractable computations of expectations.

We adopted the (SVI) in order to estimate each variational parameter in our proposed method [17] [20]. The key ideas of this inference is to consider dividing the variational variables into two subgroups: the local variables $[\Xi_l \in (\boldsymbol{Z}, \boldsymbol{\phi})]$, which are per-datapoint latent variables and the global variables $[\Xi_g \in (\boldsymbol{\gamma}, \boldsymbol{\epsilon}, \boldsymbol{\alpha}, \boldsymbol{\beta})]$, which potentially control all the data. The ith local variable Z_{ik} of the mixture component, which represents the allocation situation of sample i, is governed by the local variational parameter r_{ik}. In addition, the local variational parameter f_{ij} is proposed to capture the ith local variable ϕ_{ij} that represents the selection situation of the jth OTU in the ith community. The coordinate ascent algorithm was considered to overcome the optimization problems of these variational variables [16] [17]. The main ideas of this approach is to optimize each factor of the mean field variational distribution while fixing the others. Then, the logarithm of optimal value of $q(Z_{ik})$

is proportional to the expected logarithm of the joint distribution as follows:

$$
\begin{aligned}
&\log q^{*}\left(Z_{ik}\right) \\
&\propto \sum_{j=1}^{S} \mathrm{E}_{q}\left[\phi_{ij}\right]\left(\mathrm{E}_{q}\left[\log\left(\frac{\Gamma\left(\sum_{j=1}^{S}\alpha_{kj}\right)}{\Gamma\left(\sum_{j=1}^{S}X_{ij}+\sum_{j=1}^{S}\alpha_{kj}\right)}\right)\right]\right) \\
&+\sum_{j=1}^{S} \mathrm{E}_{q}\left[\phi_{ij}\right]\left(\mathrm{E}_{q}\left[\log\left(\frac{\Gamma\left(X_{ij}+\alpha_{kj}\right)}{\Gamma(\alpha_{kj})}\right)\right]\right) \\
&+\sum_{j=1}^{S} \mathrm{E}_{q}\left[\phi_{ij}\right]\left(\log(J_{i}!)+\log\left(\frac{1}{X_{ij}!}\right)\right) \\
&+\mathrm{E}_{q}\left[\log(\gamma_{k})\right]+\sum_{k'=1}^{k-1}\mathrm{E}_{q}\left[\log(1-\gamma_{k'})\right]
\end{aligned}
\tag{9}
$$

Because γ_k follows Beta distribution, we can obtain the analytically tractable solutions for $\mathrm{E}_q\left[\log(\gamma_k)\right]$ and $\mathrm{E}_q\left[\log(1-\gamma_{k'})\right]$. However, the first and second terms of equation (9) do not have the same forms as the logarithm of the Dirichlet prior distribution. Thus, we could not obtain directly the analytically tractable solutions. The intractable computation of expectations could be resolved by the Metropolis–Hastings algorithms and numerical integration. Nevertheless, the simulation approaches significantly increased the computational burden in a huge dimensionality of microbial metagenomics data sets [5]. Therefore, we adopted the Taylor expansion to obtain the nearly optimal analytically tractable solutions for the first and second terms of equation (9), such that the computational burdens were avoided [30] [23] [24]. The nearly optimal analytically tractable value of $q\left(\phi_{ij}\right)$ could be obtained by the proposed approach. The mathematical details of the Taylor expansion and variational objective function are specifically explained in the Supplementary Material.

The global variational parameters $\left[\Theta_g \in \left(\vartheta_k, \vartheta_k^{'}, \xi^{*}, \lambda_{kj}^{*}, \iota_j^{*}\right)\right]$ are proposed to govern the global variables Ξ_g. The SVI approach uses the stochastic gradient ascent in order to estimate the global variational parameters [17]. Furthermore, the natural gradients are adopted to account for the geometric structure of probability parameters [31] [32] [33]. It is noteworthy that the natural gradients not only are cheaper computations but also have faster convergence than standard gradients. The SVI is based on the stochastic approximation approach to iteratively generate the subsampled data sets that are used to update the values of the local and global variational parameters. The main advantages of these computational strategies is that they guarantee algorithms that avoid shallow local optima of complex objective functions.

In the case of the infinite DMM model, we generated a uniform a data set $\left[\overrightarrow{X_n}^{(N)}, \overrightarrow{Z_n}^{(N)}, \overrightarrow{\phi_n}^{(N)}\right]$ that was formed by N replicated from the microbiome community sample $\overrightarrow{X_i}$, allocation variable $\overrightarrow{Z_i}$, and indicator variable $\overrightarrow{\phi_i}$ at each iteration. Next, the noisy estimates of the natural gradient were computed with respect to each global variational parameter Θ_g given N replicates of the sampled data point. By using these gradients, the values of Θ_g were updated at each t iterations given

the local variational parameters $[\Theta_l \in (r_{ik}, f_{ij})]$ as follows:

$$\widehat{\nabla_{\Theta_g}}\mathcal{L} = \text{prior} + N\left(\mathrm{E}_{\Theta_l}\left[t\left(\overrightarrow{X_n}, \overrightarrow{Z_n}, \overrightarrow{\phi_n}\right), 1\right]\right) - \Theta_g$$
$$\Theta_g^{(t)} = \Theta_g^{(t-1)} + \rho_t \widehat{\nabla_{\Theta_g}}\mathcal{L}$$

where t(.) denotes the sufficient statistics in the exponential family and ρ_t denotes the step size at iteration t. Owing to the subsampling strategies, the SVI significantly accelerated the computational processes by avoiding the expensive sums in the ELBO when the dimensionality of the microbial metagenomics was large. The mathematical explanations of the SVI are described specifically in the Supplementary Material.

Criteria to evaluate the performance of the approaches

We used the Adjusted Rand Index (ARI) [34] in order to measure the similarity between truth (or known) clusters and clusters inferred by the various algorithms. Given a dataset of $\boldsymbol{X}$ of n total samples, $\boldsymbol{Z} = [Z_1, \ldots, Z_k]$ denoted truth cluster memberships of $\boldsymbol{X}$ into k clusters, and $\boldsymbol{Z'} = [Z'_1, \ldots, Z'_{k'}]$ denoted an inferred cluster memberships of $\boldsymbol{X}$ into k' clusters. The Rand Index (RI) was calculated as follows:

$$R\left(\boldsymbol{Z}, \boldsymbol{Z'}\right) = \frac{a+b}{n\left(n-1\right)/2}$$

where a denotes the number of times in which a pair of samples was assigned to the a same cluster in $\boldsymbol{Z}$ and the same cluster in $\boldsymbol{Z'}$ and b denotes the number of times a pair of samples that was assigned to different clusters in $\boldsymbol{Z}$ and a different clusters in $\boldsymbol{Z'}$. The values of the RI were in the range [0,1], where 1 represented a perfect similarity between truth clusters and inferred clusters. The ARI was proposed to normalize the difference between the RI and its expected value as follows:

$$\text{ARI} = \frac{RI - \mathrm{E}(RI)}{\max(RI) - \mathrm{E}(RI)}$$

where $\mathrm{E}(RI)$ was the expected value of the RI.

Database description

Tottori, Japan study

Field experiment

One hundred and ninety-eight soybean accessions registered in the National Agriculture and Food Research Organization Genebank (https://www.gene.affrc.go.jp/) were employed. The field trial was conducted in 2018 in an experimental field with sandy soil at the Arid Land Research Center, Tottori University (35°32' N lat, 134°12' E long, 14 m above sea level). Each plot consisted of four plants, and the distances between two rows, two plots, and two individuals were 50 cm, 80 cm, and 20 cm, respectively. Sowing was performed at the beginning of July, followed by thinning after 2 weeks. Fertilizer (15, 6.0, 20, 11, and 7.0 g m-2 of N, P, K, Mg, and Ca, respectively) was applied to the field before sowing. White mulching sheets (Tyvek, Dupond, USA) were laid to prevent rainwater infiltration to control

soil conditions with artificial irrigation. Watering tubes were installed under the sheets to irrigate the field. Two watering treatments, no-watered treatment and well-watered treatments, were set to evaluate the influence of drought and control conditions. Watering treatment started after thinning every year, which was 2 weeks after sowing. Artificial irrigation was applied for 5 hours daily (7:00–9:00, 12:00–14:00, 16:00–17:00).

DNA extraction

DNA extraction was performed using our custom protocol with magnetic beads [35]. Briefly, the collected root tissues were ground to a fine powder using a Multi-Beads Shocker (MB2200(S), Yasui Kikai Co. Osaka, Japan). For each of the collected tissue samples, 500 mg of the powdered sample was transferred into a 1.5 mL tube cooled by liquid nitrogen. One mL of lysate binding buffer (1 M LiCl Sigma-Aldrich, Cat. #L7026-500ML; 100 mM Tris-HCl, Wako, Cat. #318-90225; 1% SDS, Wako, Cat. #313-90275; 10 mM EDTA pH 8.0, Wako, Cat. #311-90075; Antifoam A, Sigma-Aldrich, Cat. #A5633-25G; 5 mM DTT, Wako, Cat. #048-29224; 11.2 M 3-Mercapto-1,2-propanediol, Wako, Cat. #139-16452; DNase/RNase-free H2O, Thermo Fisher Scientific, Cat. #10977015) [36] was added to the sample, which was then homogenized by vortexing, followed by incubation at room temperature (22°C) for 5 min. The tube was centrifuged at 15,000 rpm for 10 min at room temperature, and the supernatant was transferred to a new 1.5 mL tube. Fifty μL of LBB lysate was put into 1.5 mL tubes, and an equal amount of AMPure XP beads was added, followed by incubation at room temperature for 5 min after vortexing. The mixture was placed on a magnetic station for 5 min, and the supernatant was removed. The magnetic beads were washed twice with 200 μL of 80% ethanol. Finally, DNA was eluted with 20 μL of 10 mM Tris-HCl (pH 7.5).

16S rRNA gene amplicon sequencing

Library preparation using a two-step PCR amplification protocol was reported in our previous publication [35, 36]. Briefly, the V4 region of bacterial 16S rRNA gene was amplified with 515f and 806rB primers (forward primer: 5'- TCG TCG GCA GCG TCA GAT GTG TAT AAG AGA CAG- [3–6-mer Ns] – GTG YCA GCM GCC GCG GTA A -3'; reverse primer: 5'- GTC TCG TGG GCT CGG AGA TGT GTA TAA GAG ACA G [3–6-mer Ns] - GGA CTA CNV GGG TWT CTA AT -3') [37, 38]. Each sample (1 μL of 10-fold diluted DNA) was amplified in a 10 μL reaction volume containing 0.2 U KOD FX Neo DNA polymerase (TOYOBO Co., Ltd., Osaka, Japan), 2 × PCR buffer (TOYOBO), 0.4 mM dNTPs (TOYOBO), 0.2 μM forward and reverse primers, and 1 μM blocking primers (mPNA and pPNA, PNA BIO, Inc., Newbury Park, CA). PCR was performed using the following specifications: 94°C for 2 min followed by 35 cycles at 98°C for 10 s, 78°C for 10 s, 55°C for 30 s, 68°C for 50 s, and a final extension at 68°C for 5 min (ramp rate = 1°C/s).

The first PCR products was then purified with a mixture of exonuclease and alkaline phosphatase. Two μL of ExoSAP-IT Express (Thermo Fisher Scientific, Cat #75001.1.EA) was added to 5 μL of the product obtained from the first PCR, and the mixture was incubated at 37°C for 4 min, followed by 80°C for 1 min.

The second PCR was carried out with the following primers: forward primer: 5'- AAT GAT ACG GCG ACC ACC GAG ATC TAC AC - [8-mer index] - TCG TCG GCA GCG TC -3', and reverse primer: 5'- CAA GCA GAA GAC GGC ATA CGA

GAT - [8-mer index] - GTC TCG TGG GCT CGG -3' (Toju and Baba, 2018). Each sample (0.8 μL of purified product from the first PCR) was amplified in a 10 μL reaction volume containing 0.2 U KOD FX Neo DNA polymerase (TOYOBO), 2 $\times$ PCR buffer (TOYOBO), 0.4 mM dNTPs (TOYOBO), 0.3 μM forward and reverse primers, and 1 μM blocking primers (mPNA and pPNA). PCR was performed as follows: 94°C for 2 min, followed by 8 cycles at 98°C for 10 s, 78°C for 10 s, 55°C for 30 s, 68°C for 50 s, and a final extension at 68°C for 5 min (ramp rate = 1°C/s). Following amplification, PCR products for each sample were cleaned and size-selected using AMPure XP beads and washed twice with 80% ethanol. The libraries were eluted from the pellet with 10 μL of 10 mM Tris-HCl pH 7.5, quantified with a microplate photometer (Infinite 200 PRO M Nano+, TECAN Japan Co., Ltd.), and pooled into a single library in equal molar quantities. The pooled library was sequenced on an Illumina MiSeq platform using a 2$\times$ 300-bp MiSeq Reagent Nano Kit v3 (Illumina, CA, USA).

Taxonomic profiling and data preprocessing

Sequencing primers and short (<150 bp) reads were removed with Cutadapt v.1.18. The primer-free FASTQ files were further processed using R v3.6.0 with DADA2 v.1.14.0 [39]. First, the FASTQ file was trimmed. We applied the parameter with truncation length of 240 for forward and 160 for reverse reads. These reads underwent further quality filtering as error rates were calculated and removed from the dereplicated reads. The forward and reverse sequences were then merged with each other. Next, potentially chimeric sequences and sequencing errors were removed. Taxonomy was assigned using the SILVA v.132 training set [40]. The filtered matrix was rarefied to 3,000 reads per sample using the vegan 2.5-6 package [41], and then used to calculate Bray-Curtis distance. We denoted Data set A as our Tottori data set.

Study inclusion and data acquisition

We also employed the case–control 16S amplicon sequencing from three published human microbiome data sets spanning three different disease states: *Clostridium difficile* infection (CDI) [25], inflammatory bowel disease (IBD) [27], and obesity (OB) [26]. These data sets are available from the MicrobiomeHD database [42]. Dataset B represented the CDI data set that included a total of 183 diarrheal stool samples from the 94 individuals with CDI, 89 diarrheal control samples, 155 non-diarrheal control stool samples, and 3,347 microbiome species (or OTUs). Dataset C represented the IBD data set that included 146 IBD case samples, 16 non-IBD control samples and 10,119 microbiome species (or OTUs). Finally, Dataset D represented the OB dataset that was the most challenging and largest one. There were 1,081 fecal samples from 977 individuals and 55,964 microbiome species (or OTUs).

Open-source software

Our software was implemented in Python. It used some standard libraries, such as NumPy and SciPy, for mathematical computations. It inputs microbiome counts data in a csv file and output the inferred clusters and a core set of selected OTUs. The main options in the software tool are a maximum number of clusters that pose

limitations in estimating the number of clusters, a number of OTUs that users want to select. We kept the convergence criterion fixed across all data sets in this study. The SVVS algorithm stopped when the change in ELBO computations was less than 1e-3. For datasets notably smaller or larger in scale than what we considered in this study, the number of iterations was modified. This is a tunable option in the software. Our software is available at https://github.com/tungtokyo1108/SVVS

Results

Runtime performance and physical memory of the computational system

An important advantage of the SVVS over conventional DMM approaches is that the computational time and memory required for the calculations can be greatly reduced. To evaluate the computational time and memory of the different approaches, we diversified the sample sizes and numbers of OTUs in the example data sets. The scalability of the methods was specifically demonstrated in cases of datasets C and D; meanwhile, datasets A and B were selected to compare their accuracies. We followed the Laplace approximation to the model evidence and default values of the DirichletMultinomial 1.34.0 package in R in order to determine the number of clusters K for the finite DMM model [5] [43]. Our proposed method does not require choosing the number of clusters, because the number of clusters is an estimate as a random variable. Our Python implementations of the SVVS for the infinite DMM model were used to analyze all real data sets. Tables 1 and 2 compared the computational time and physical memory required for the calculation between the SVVS algorithm of the infinite DMM model and the EM algorithm of the finite DMM model. We found that the SVVS was able to reduce run times and physical memories considerably for data set A, B, and C. The SVVS was the only approach that was able to analyze dataset D, which was a large data set of more than 50,000 OTUs and 1,000 samples. Besides, the time complexity and memories of each of the above methods, were found to increase regularly with the numbers of OTUs and the number of samples. The SVVS used the iterative optimization algorithms to estimate the parameters; thus, a convergence criterion was used to implement a stopping rule (Supplementary Material).

The SVVS improves accuracy of performance of the approach

Table 3 compares the values of the ARI between two methods. The SVVS algorithm of the infinite DMM model demonstrated a better performances than the conventional finite DMM model for all real data sets. Specifically, the SVVS showed the highest ARI value (ARI = 0.98) in the case of Dataset A; meanwhile, the ARI value of the finite DMM with the EM algorithm was 0.56. In the case of Dataset B, the ARI values slightly reduced in the performance of the SVVS (ARI = 0.66) and EM algorithms (ARI = 0.44). The number of OTUs in Dataset B (3,347 OTUs) was significantly larger than that in Dataset A (888 OTUs). The small sample size and the large number of OTUs on Dataset C considerably influenced the performances of the two approaches. The lowest ARI values were shown for the SVVS (ARI = 0.48) and EM algorithms (ARI = 0.21). However, the ARI value of the SVVS approach slightly increased in the case of Dataset D when the number of samples

was increased. The EM algorithm of the finite DMM model could not complete its estimation in Dataset D, in which the dimensionality of microbial data was the highesr.

The selected microbiome species mapped on the phylogenetic trees

The other considerable contribution of SVVS is the ability to select a minimal-size core set of microbial species that shows the significant differences among the clusters obtained in the analysis. Specifically, figure 1a,b shows that the top 50 and 100 selected microbiome species in Dataset A are mapped on the 16S phylogenetic tree. Most microbiome families that had significant associations with plant growth promotion under drought were observed in the orange-colored region of the tree. Our results are in accordance with those of some previous studies. For example, a large number of species of families of bacteria, including *Micrococcaceae, Paenibacillaceae, Bacillaceae* and *Planococcaceae*, showed a strong dominance in ecosystems after the impact of wildfires on living organisms [44].

Moreover, figure 2 shows that the top 100 selected microbiome species in Dataset B are mapped on the 16S phylogenetic tree. The green-colored region of the tree includes most of the microbiome species that show significant associations with non-diarrheal controls. A number of dominant species that were significantly associated with the CDI case was observed in the orange-colored region of the tree. Meanwhile a mixture of the two groups was observed in the purple region. Specifically, a large number of microbiome species belonged to *Bacteroidaceae, Porphyromonadaceae*, and *Rikenellaceae* families observed in the green-colored region of the tree. A number of studies have shown that several bacterial species within these families are largely absent in CDI cases and closely associated with non-diarrheal controls [25, 45]. One of the main risk factors is the antibiotic treatments that alter the host nutritional landscape in order to produce the essential branched-chain amino acids and proline for *C. difficile* growth and to suppress the return of members from the *Rikenellaceae, Bacteroidaceae* families [46, 47].

Discussion and conclusion

The rapid identification of the minimal-size core set of OTUs in the high-dimensional data of microbial studies is essential to further our understanding of structures of microbial communities in clustering analysis. The intensive concentration on a small number of relevant OTUs that significantly contribute to the task of clustering will not only increase the performance of these analyse but also open up new opportunities for studies that explore the important associations of microbial communities on human diseases, precision medicine, and environmental conditions.

Since the substantial increase in dimensionality of the microbial datasets causes computational burden and poor performance of previous methods, the proposed approach could satisfy the high demands in the microbiome analysis. Our SVVS approach was useful in several respects. First, the SVVS integrated an indicator variable into the framework of the infinite DMM model to identify the significant microbiome species (or OTUs) and used the SVI to overcome the computational limitations. Thus, the SVVS approach quickly identified the core set of microbial species (or OTUs), which considerably improved the performance of the infinite DMM model. In particular, the SVVS method could complete its main tasks in the

massive microbiome datasets [26] that the previous methods could not do. Second, the stick-breaking representation was proposed to extend the finite DMM model to the infinite case. This solution treated the total number of clusters as a free parameter of the model that could help avoid the disadvantages of determining the number of clusters before running the algorithms.

In recent years, a number of studies have highlighted a substantial role of large-scale analysis in discovering the microbiome connections with host metabolism, host genetics in human health, medication [48, 49] and an agroecosystem [36]. An increasing number of multi-omics datasets have been published, such as the integration of metagenomics, metatranscriptomics, and metaproteomics [50] or whole-genome sequencing and whole-transcriptome sequencing of TCGA cancer microbiome [51]. In the future, we plan to extend the SVVS approach to the comprehensive analysis of multi-omics datasets. The main framework of the SVVS method can be developed for the other Bayesian mixture models, such as beta-mixture models, for microarray gene expression datasets [52] or the multinomial mixture model for ChIP-exo sequencing data [53]. Therefore, it provides to new opportunities for discovering the significant associations of microbes with specific nutrients and medication or the important interactions between plants, microbes, and soils. Moreover, the dimensionality of databases significantly increased when other datasets were combined with microbiome data. We considered the integration of the strategies of parallel computations that can partition the data both horizontally (over sample) and vertically (over features) in order to speed up the computational processes [54].

Acknowledgements
We are grateful to the technical staff of Arid Land Research Center, Tottori University, and Izumi Higashida for management of the field experiment of soybean. We would like to thank all the members of JST-CREST Program including Mikio Nakazono, Hirokazu Takahashi, Toru Fujiwara, Yoshihiro Ohmori, Hideki Takanashi, Akito Kaga, Mai Tsuda, Yuji Sawada for conducting the field experiment.

Funding
This work was supported by JSPS KAKENHI Grant Number JP21J21850, JST-CRESET Program Grant Number JPMJCR1602 and JST-Mirai Program Grant Number JPMJMI120C7, Japan.

Availability of data and materials
https://github.com/tungtokyo1108/SVVS

Ethics approval and consent to participate
Not applicable

Competing interests
The authors declare that they have no competing interests.

Consent for publication
Not applicable.

Authors' contributions
TD and HI designed the study. YT, YY, HT and HI designed and conducted the field experiment in Tottori. KK, EU, SK, TS and YI performed the microbiome analysis from tissue sampling, library preparation, sequencing, and primary informatics for taxonomic assignment and diversity statistics. TD developed the method and analyze the data. TD and HI interpreted the data and wrote the manuscript. The authors read and approved the final manuscript.

Authors' information
Text for this section...

Author details
[1]Graduate School of Agricultural and Life Sciences, The University of Tokyo, Tokyo, Japan. [2]RIKEN BioResource Research Center, Tsukuba, Ibaraki, Japan. [3]Arid Land Research Center, Tottori University, Tottori, Japan.

References

1. Visconti, A., Le Roy, C.I., Rosa, F., Rossi, N., Martin, T.C., Mohney, R.P., Li, W., de Rinaldis, E., Bell, J.T., Venter, J.C., *et al.*: Interplay between the human gut microbiome and host metabolism. Nature communications **10**(1), 1–10 (2019)
2. Al Nabhani, Z., Eberl, G.: Imprinting of the immune system by the microbiota early in life. Mucosal immunology **13**(2), 183–189 (2020)
3. Emerson, J.B., Roux, S., Brum, J.R., Bolduc, B., Woodcroft, B.J., Jang, H.B., Singleton, C.M., Solden, L.M., Naas, A.E., Boyd, J.A., *et al.*: Host-linked soil viral ecology along a permafrost thaw gradient. Nature microbiology **3**(8), 870–880 (2018)
4. Caporaso, J.G., Kuczynski, J., Stombaugh, J., Bittinger, K., Bushman, F.D., Costello, E.K., Fierer, N., Peña, A.G., Goodrich, J.K., Gordon, J.I., *et al.*: Qiime allows analysis of high-throughput community sequencing data. Nature methods **7**(5), 335–336 (2010)
5. Holmes, I., Harris, K., Quince, C.: Dirichlet multinomial mixtures: generative models for microbial metagenomics. PloS one **7**(2), 30126 (2012)
6. Depner, M., Taft, D.H., Kirjavainen, P.V., Kalanetra, K.M., Karvonen, A.M., Peschel, S., Schmausser-Hechfellner, E., Roduit, C., Frei, R., Lauener, R., *et al.*: Maturation of the gut microbiome during the first year of life contributes to the protective farm effect on childhood asthma. Nature Medicine **26**(11), 1766–1775 (2020)
7. Vieira-Silva, S., Falony, G., Belda, E., Nielsen, T., Aron-Wisnewsky, J., Chakaroun, R., Forslund, S.K., Assmann, K., Valles-Colomer, M., Nguyen, T.T.D., *et al.*: Statin therapy is associated with lower prevalence of gut microbiota dysbiosis. Nature **581**(7808), 310–315 (2020)
8. Hughes, D.A., Bacigalupe, R., Wang, J., Rühlemann, M.C., Tito, R.Y., Falony, G., Joossens, M., Vieira-Silva, S., Henckaerts, L., Rymenans, L., *et al.*: Genome-wide associations of human gut microbiome variation and implications for causal inference analyses. Nature microbiology **5**(9), 1079–1087 (2020)
9. Zaneveld, J.R., McMinds, R., Thurber, R.V.: Stress and stability: applying the anna karenina principle to animal microbiomes. Nature microbiology **2**(9), 1–8 (2017)
10. Papaspiliopoulos, O., Roberts, G.O.: Retrospective markov chain monte carlo methods for dirichlet process hierarchical models. Biometrika **95**(1), 169–186 (2008)
11. Bouguila, N., Ziou, D.: A countably infinite mixture model for clustering and feature selection. Knowledge and information systems **33**(2), 351–370 (2012)
12. Ferguson, T.S.: A bayesian analysis of some nonparametric problems. The annals of statistics, 209–230 (1973)
13. Green, P.J., Richardson, S.: Modelling heterogeneity with and without the dirichlet process. Scandinavian journal of statistics **28**(2), 355–375 (2001)
14. Ishwaran, H., James, L.F.: Gibbs sampling methods for stick-breaking priors. Journal of the American Statistical Association **96**(453), 161–173 (2001)
15. Jordan, M.I., Ghahramani, Z., Jaakkola, T.S., Saul, L.K.: An introduction to variational methods for graphical models. Machine learning **37**(2), 183–233 (1999)
16. Blei, D.M., Jordan, M.I., *et al.*: Variational inference for dirichlet process mixtures. Bayesian analysis **1**(1), 121–143 (2006)
17. Hoffman, M.D., Blei, D.M., Wang, C., Paisley, J.: Stochastic variational inference. Journal of Machine Learning Research **14**(5) (2013)
18. Raj, A., Stephens, M., Pritchard, J.K.: faststructure: variational inference of population structure in large snp data sets. Genetics **197**(2), 573–589 (2014)
19. Gopalan, P., Hao, W., Blei, D.M., Storey, J.D.: Scaling probabilistic models of genetic variation to millions of humans. Nature genetics **48**(12), 1587 (2016)
20. Dang, T., Kishino, H.: Stochastic variational inference for bayesian phylogenetics: a case of cat model. Molecular biology and evolution **36**(4), 825–833 (2019)
21. Fourment, M., Darling, A.E.: Evaluating probabilistic programming and fast variational bayesian inference in phylogenetics. PeerJ **7**, 8272 (2019)
22. Fourment, M., Magee, A.F., Whidden, C., Bilge, A., Matsen IV, F.A., Minin, V.N.: 19 dubious ways to compute the marginal likelihood of a phylogenetic tree topology. Systematic biology **69**(2), 209–220 (2020)
23. Ma, Z., Leijon, A.: Bayesian estimation of beta mixture models with variational inference. IEEE Transactions on Pattern Analysis and Machine Intelligence **33**(11), 2160–2173 (2011)
24. Ma, Z., Rana, P.K., Taghia, J., Flierl, M., Leijon, A.: Bayesian estimation of dirichlet mixture model with variational inference. Pattern Recognition **47**(9), 3143–3157 (2014)
25. Schubert, A.M., Rogers, M.A., Ring, C., Mogle, J., Petrosino, J.P., Young, V.B., Aronoff, D.M., Schloss, P.D.: Microbiome data distinguish patients with clostridium difficile infection and non-c. difficile-associated diarrhea from healthy controls. MBio **5**(3), 01021–14 (2014)
26. Goodrich, J.K., Waters, J.L., Poole, A.C., Sutter, J.L., Koren, O., Blekhman, R., Beaumont, M., Van Treuren, W., Knight, R., Bell, J.T., *et al.*: Human genetics shape the gut microbiome. Cell **159**(4), 789–799 (2014)
27. Gevers, D., Kugathasan, S., Denson, L.A., Vázquez-Baeza, Y., Van Treuren, W., Ren, B., Schwager, E., Knights, D., Song, S.J., Yassour, M., *et al.*: The treatment-naive microbiome in new-onset crohn's disease. Cell host & microbe **15**(3), 382–392 (2014)
28. Boutemedjet, S., Bouguila, N., Ziou, D.: A hybrid feature extraction selection approach for high-dimensional non-gaussian data clustering. IEEE Transactions on Pattern Analysis and Machine Intelligence **31**(8), 1429–1443 (2008)
29. Dickey, J.M.: Multiple hypergeometric functions: Probabilistic interpretations and statistical uses. Journal of the American Statistical Association **78**(383), 628–637 (1983)
30. Wang, C., Blei, D.M.: Variational inference in nonconjugate models. Journal of Machine Learning Research **14**(4) (2013)
31. Amari, S.-I.: Differential geometry of curved exponential families-curvatures and information loss. The Annals

of Statistics, 357–385 (1982)
32. Robbins, H., Monro, S.: A stochastic approximation method. The annals of mathematical statistics, 400–407 (1951)
33. Honkela, A., Raiko, T., Kuusela, M., Tornio, M., Karhunen, J.: Approximate riemannian conjugate gradient learning for fixed-form variational bayes. The Journal of Machine Learning Research **11**, 3235–3268 (2010)
34. Rand, W.M.: Objective criteria for the evaluation of clustering methods. Journal of the American Statistical association **66**(336), 846–850 (1971)
35. Kumaishi, K., Usui, E., Suzuki, K., Kobori, S., Sato, T., Toda, Y., Takanashi, H., Shinozaki, S., Noda, M., Takakura, A., et al.: Simple amplicon sequencing library preparation for plant root microbial community profiling. bioRxiv (2021)
36. Ichihashi, Y., Date, Y., Shino, A., Shimizu, T., Shibata, A., Kumaishi, K., Funahashi, F., Wakayama, K., Yamazaki, K., Umezawa, A., *et al.*: Multi-omics analysis on an agroecosystem reveals the significant role of organic nitrogen to increase agricultural crop yield. Proceedings of the National Academy of Sciences **117**(25), 14552–14560 (2020)
37. Caporaso, J.G., Lauber, C.L., Walters, W.A., Berg-Lyons, D., Lozupone, C.A., Turnbaugh, P.J., Fierer, N., Knight, R.: Global patterns of 16s rrna diversity at a depth of millions of sequences per sample. Proceedings of the national academy of sciences **108**(Supplement 1), 4516–4522 (2011)
38. Lundberg, D.S., Yourstone, S., Mieczkowski, P., Jones, C.D., Dangl, J.L.: Practical innovations for high-throughput amplicon sequencing. Nature methods **10**(10), 999–1002 (2013)
39. Callahan, B.J., McMurdie, P.J., Rosen, M.J., Han, A.W., Johnson, A.J.A., Holmes, S.P.: Dada2: high-resolution sample inference from illumina amplicon data. Nature methods **13**(7), 581–583 (2016)
40. Quast, C., Pruesse, E., Yilmaz, P., Gerken, J., Schweer, T., Yarza, P., Peplies, J., Glöckner, F.O.: The silva ribosomal rna gene database project: improved data processing and web-based tools. Nucleic acids research **41**(D1), 590–596 (2012)
41. Oksanen, J., Blanchet, F., Friendly, M., Kindt, R., Legendre, P., McGlinn, D., et al.: vegan: community ecology package. R package version 2.5-7. 2020
42. Duvallet, C., Gibbons, S.M., Gurry, T., Irizarry, R.A., Alm, E.J.: Meta-analysis of gut microbiome studies identifies disease-specific and shared responses. Nature communications **8**(1), 1–10 (2017)
43. Morgan, M.: Dirichletmultinomial: Dirichlet-multinomial mixture model machine learning for microbiome data. R package version 1.34.0 **1**(0) (2021)
44. de Miera, L.E.S., Pinto, R., Gutierrez-Gonzalez, J.J., Calvo, L., Ansola, G.: Wildfire effects on diversity and composition in soil bacterial communities. Science of the Total Environment **726**, 138636 (2020)
45. Rousseau, C., Poilane, I., De Pontual, L., Maherault, A.-C., Le Monnier, A., Collignon, A.: Clostridium difficile carriage in healthy infants in the community: a potential reservoir for pathogenic strains. Clinical Infectious Diseases **55**(9), 1209–1215 (2012)
46. Hofmann, J.D., Otto, A., Berges, M., Biedendieck, R., Michel, A.-M., Becher, D., Jahn, D., Neumann-Schaal, M.: Metabolic reprogramming of clostridioides difficile during the stationary phase with the induction of toxin production. Frontiers in microbiology **9**, 1970 (2018)
47. Fletcher, J.R., Pike, C.M., Parsons, R.J., Rivera, A.J., Foley, M.H., McLaren, M.R., Montgomery, S.A., Theriot, C.M.: Clostridioides difficile exploits toxin-mediated inflammation to alter the host nutritional landscape and exclude competitors from the gut microbiota. Nature Communications **12**(1), 1–14 (2021)
48. Kurilshikov, A., Medina-Gomez, C., Bacigalupe, R., Radjabzadeh, D., Wang, J., Demirkan, A., Le Roy, C.I., Garay, J.A.R., Finnicum, C.T., Liu, X., *et al.*: Large-scale association analyses identify host factors influencing human gut microbiome composition. Nature Genetics **53**(2), 156–165 (2021)
49. Asnicar, F., Berry, S.E., Valdes, A.M., Nguyen, L.H., Piccinno, G., Drew, D.A., Leeming, E., Gibson, R., Le Roy, C., Al Khatib, H., *et al.*: Microbiome connections with host metabolism and habitual diet from 1,098 deeply phenotyped individuals. Nature Medicine **27**(2), 321–332 (2021)
50. Hultman, J., Waldrop, M.P., Mackelprang, R., David, M.M., McFarland, J., Blazewicz, S.J., Harden, J., Turetsky, M.R., McGuire, A.D., Shah, M.B., *et al.*: Multi-omics of permafrost, active layer and thermokarst bog soil microbiomes. Nature **521**(7551), 208–212 (2015)
51. Poore, G.D., Kopylova, E., Zhu, Q., Carpenter, C., Fraraccio, S., Wandro, S., Kosciolek, T., Janssen, S., Metcalf, J., Song, S.J., *et al.*: Microbiome analyses of blood and tissues suggest cancer diagnostic approach. Nature **579**(7800), 567–574 (2020)
52. Ji, Y., Wu, C., Liu, P., Wang, J., Coombes, K.R.: Applications of beta-mixture models in bioinformatics. Bioinformatics **21**(9), 2118–2122 (2005)
53. Yamada, N., Lai, W.K., Farrell, N., Pugh, B.F., Mahony, S.: Characterizing protein–dna binding event subtypes in chip-exo data. Bioinformatics **35**(6), 903–913 (2019)
54. Xing, E.P., Ho, Q., Xie, P., Wei, D.: Strategies and principles of distributed machine learning on big data. Engineering **2**(2), 179–195 (2016)

Figures

Figure 1 The microbial species selected by the SVVS approach are mapped on the phylogenetic tree in the case of Dataset A; **a.** Mapping of 50 selected microbiome species; **b.** Mapping of 100 selected microbiome species

Note: The red-colored plus symbol denotes the control and the blue-colored star denotes drought

Figure 2 The microbial species selected by the SVVS approach are mapped on the phylogenetic tree in the case of Dataset B (CDI disease)
Note: The red-colored plus symbol denotes for CDI cases and the blue-colored star denotes non-diarrheal control

Table 1 Running time of the two approaches on the real data sets

	Finite DMM with EM algorithm	Infinite DMM with SVVS algorithm
Dataset A	17.63 min	2.68 min
Dataset B	2.75 h	13.25 min
Dataset C	3.37 d	30 min
Dataset D	Failed	5 h

Table 2 Physical memories of the two approaches on the real datasets

	Finite DMM with EM algorithm	Infinite DMM with SVVS algorithm
Dataset A	1.02 Gbs	0.186 Gbs
Dataset B	3.5 Gbs	1.65 Gbs
Dataset C	15 Gbs	4.5 Gbs
Dataset D	over 128 Gbs	45 Gbs

Table 3 ARI scores of the two approaches on the real data sets

	Finite DMM with EM algorithm	Infinite DMM with SVVS algorithm
Dataset A	0.56	0.98
Dataset B	0.44	0.66
Dataset C	0.21	0.48
Dataset D	Failed	0.5

Tables
Additional Files
Additional file 1: Supplemental Materials and Methods.

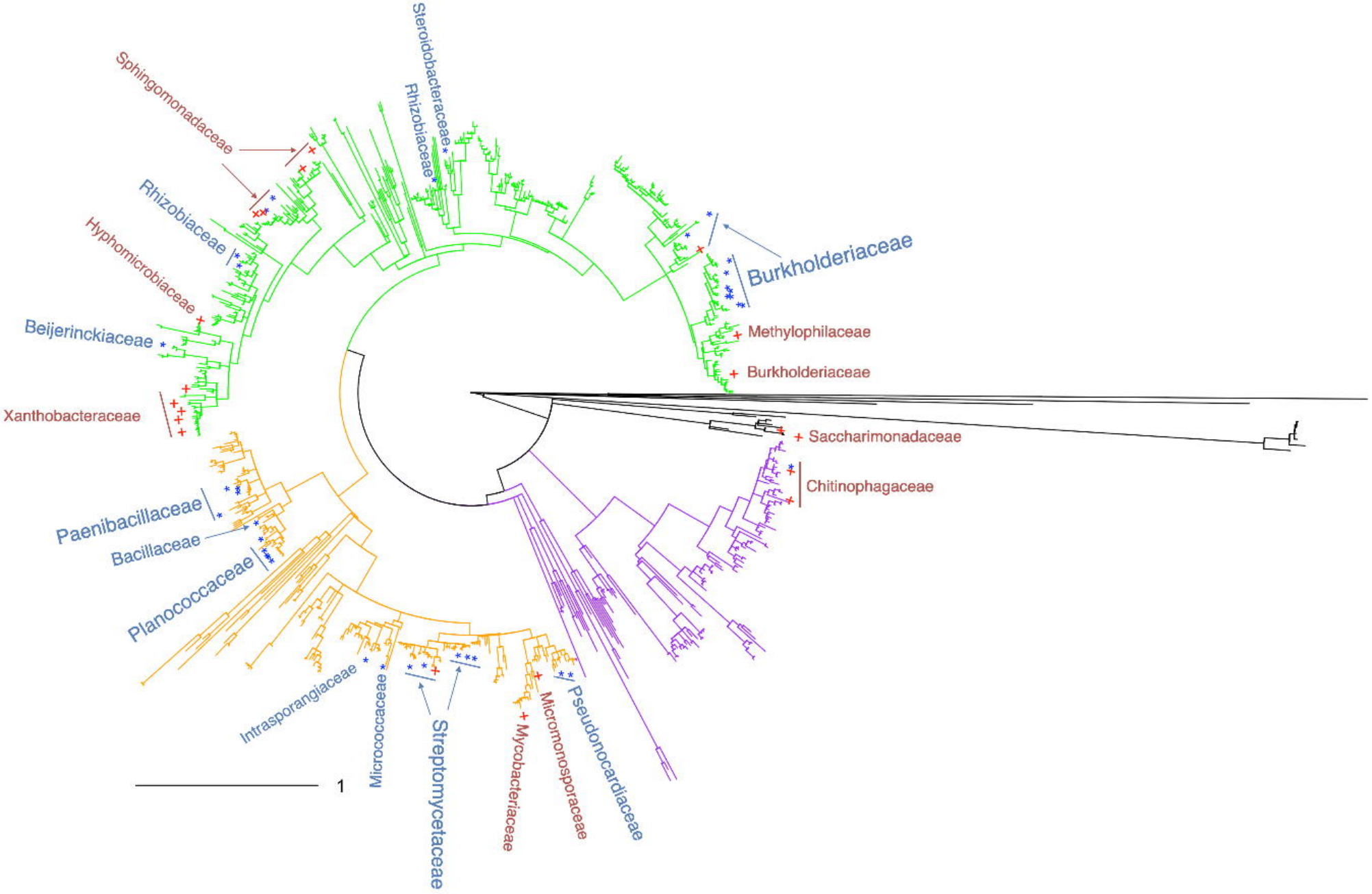
Sphingomonadaceae
Steroidobacteraceae
Rhizobiaceae
Rhizobiaceae
Hyphomicrobiaceae
Beijerinckiaceae
Xanthobacteraceae
Burkholderiaceae
Methylophilaceae
Burkholderiaceae
Saccharimonadaceae
Chitinophagaceae
Paenibacillaceae
Bacillaceae
Planococcaceae
Intrasporangiaceae
Micrococcaceae
Streptomycetaceae
Mycobacteriaceae
Micromonosporaceae
Pseudonocardiaceae
1

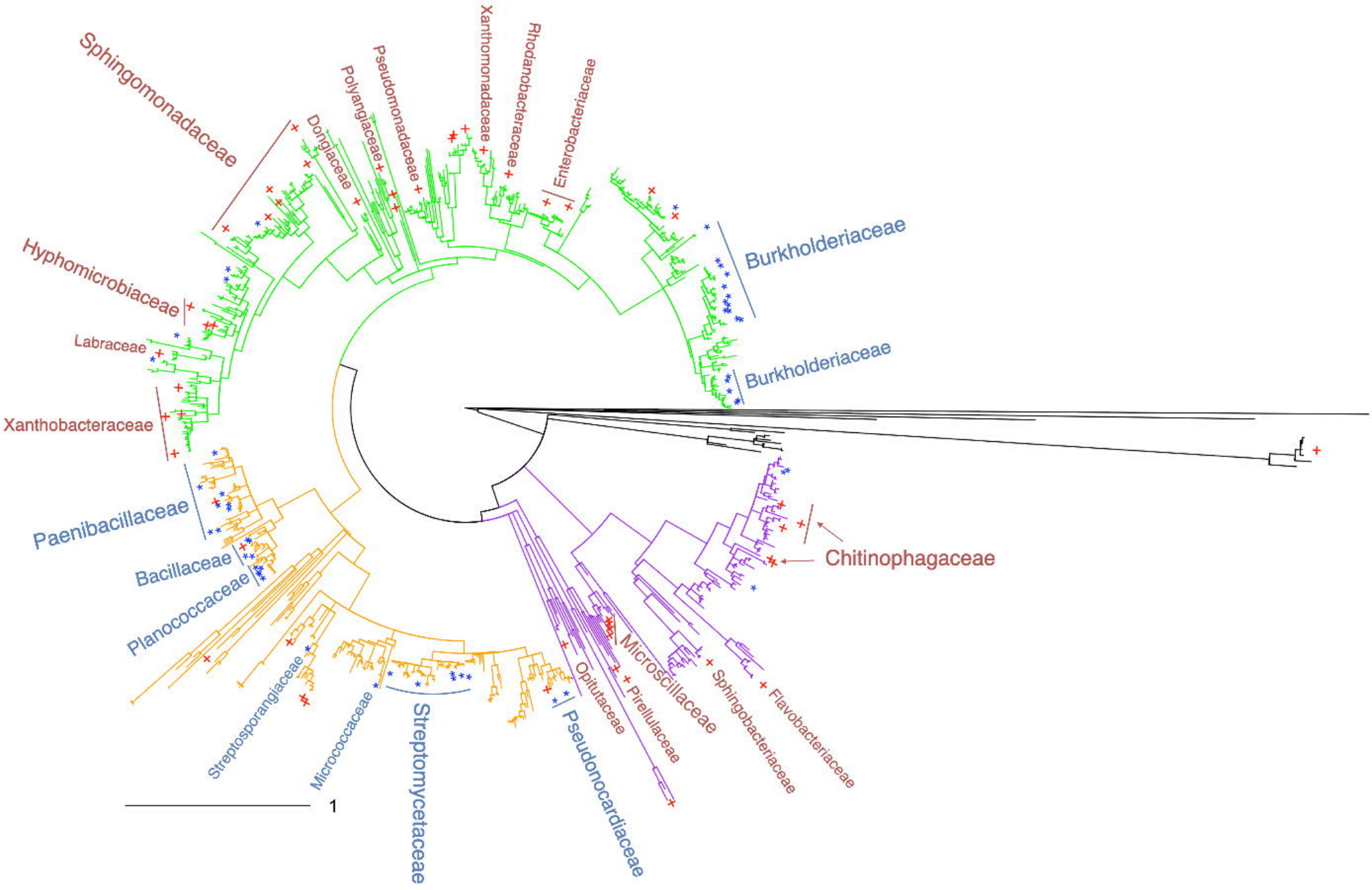
Sphingomonadaceae
Hyphomicrobiaceae
Labraceae
Xanthobacteraceae
Paenibacillaceae
Bacillaceae
Planococcaceae
Streptosporangiaceae
Micrococcaceae
Streptomycetaceae
Pseudonocardiaceae
Opitutaceae
Pirellulaceae
Microscillaceae
Sphingobacteriaceae
Flavobacteriaceae
Chitinophagaceae
Burkholderiaceae
Burkholderiaceae
Enterobacteriaceae
Rhodanobacteraceae
Xanthomonadaceae
Pseudomonadaceae
Polyangiaceae
Dongiaceae
1

Bacteroidaceae
Porphyromonadaceae
Bacteroidaceae
Bacteroidaceae
Rikenellaceae
Lachnospiraceae
Ruminococcaceae
Enterobacteriaceae
Enterococcaceae
Lactobacillaceae
Veillonellaceae
5